THREE-DIMENSIONAL REVERSED-CYCLIC ANALYSIS OF REINFORCED CONCRETE MEMBERS USING THE MICROPLANE MODEL

DREIDIMENSIONALE ZYKLISCHE ANALYSE VON STAHLBETON-BAUTEILEN MIT DEM MICROPLANE MODELL

ANALYSE TRI-DIMENSIONNELLE CYCLIQUE INVERSE, PAR LA METHODE MICROPLANE, DE POUTRES EN BETON RENFORCE

Matthew Hoehler, Joško Ožbolt

SUMMARY

This paper presents the current state of the microplane based finite element analysis program MASA for three-dimensional, nonlinear, reversed-cyclic analysis of reinforced concrete members. The program's performance is assessed by comparison with experimental work performed previously at the University of California, Berkeley. The program is shown to accurately represent global hysteretic behaviour up to failure for cases with a limited number of cycles, while simultaneously providing information about local behaviour such as concrete cracking and steel to concrete bond interaction. The performance achieved using this approach is discussed in the context of the model sophistication required to obtain the results.

ZUSAMMENFASSUNG

In dem vorliegenden Bericht sind die Ergebnisse der dreidimensionalen nichtlinearen FE Berechnungen von Bauteilen aus Stahlbeton unter der zyklischen Beanspruchung dargestellt. Es wurde das Programm MASA, das auf dem „Microplane" Modell für Beton basiert, verwendet. Die Ergebnisse der numerischen Untersuchungen wurden mit den experimentellen Untersuchungen, die an der Universität von Kalifornien (Berkeley) durchgeführt wurden, verglichen. Es wird gezeigt, dass für eine begrenzte Anzahl der Lastzyklen das Programm MASA in der Lage ist, das globale Verhalten der Bauteile realistisch abzubilden. Weiterhin wird über die Verwendung der verschmierten Rissmethode bei der Modellierung von zyklischen Beanspruchungen als auch über die Vorschläge für die weitere Untersuchungen und Verbesserungen des Modells diskutiert.

RESUME[1]

Cette publication présente les développements les plus récents de l'analyse tri-dimensionnelle non-linéaire cyclique inverse de poutres en béton renforcé, a l'aide du logiciel d'analyse par éléments finis, MASA. Les résultats de performance sont comparés a ceux de travaux antérieurs experimentaux conduits par l'Université de Califonie (Berkeley). Le logiciel MASA simule de facon précise un comportement d'hystérésie globale jusqu'au point de rupture pour les cas comprenants un nombre fini de cycles. Ce logiciel fournit également des informations de nature locale sur le comportement de fissures, et de l'interaction acier/beton. La qualité des résultats obtenus par cette approche est évaluée en prenant compte du degré de sophistication requis du modèle pour presenter des résultats interessants.

KEYWORDS: microplane model, cyclic analysis, reinforced concrete

INTRODUCTION

MASA is a Finite Element Method (FEM) based computer program capable of three-dimensional (3D), fully nonlinear analysis of concrete and concrete-like materials and reinforced concrete structures. The program is based on the microplane model with relaxed kinematic constraint, which is a continuum-based model that incorporates damage at the material level [Ožbolt et al. 2001]. MASA has hereto been shown to perform exceptionally well in "blind" comparisons with available commercial and research finite element codes for simulation of pre- and post-peak behaviour of monotonically loaded concrete and reinforced concrete [EDF 2001], [Ožbolt et al. 2000]. While the microplane material formulations are capable of 3D cycling, few applications to practical problems with reversed-cyclic loading exist [Ožbolt et al. 1998].

This paper presents results from a numerical investigation of two reinforced concrete beam members that were previously tested by Ma et al. at the University of California, Berkeley [Ma et al. 1976].

[1] The authors would like to thank Gregoire Landel and Marc Trotoux for translating the summary to french.

The ability of MASA to accurately capture global hysteretic behaviour is demonstrated. The primary advantages over other analytical approaches for cyclic analysis of reinforced concrete are:

- the element and material formulations are 3D and thus applicable for any loading combination,
- local behaviour, such as concrete cracking and steel strain distribution, can be qualitatively and quantitatively investigated,
- effects of shear are automatically included.

The cost of these advantages is that the analysis is relatively computationally expensive and thus limited to structural components, e.g. single members, beam-column joints, beam-slab connections, etc., with the currently available computers and the existing solution strategies implemented in MASA. Furthermore, the investigation illustrates that when such a sophisticated analysis approach is taken, the accurate representation of boundary conditions is critical.

MATERIAL MODELS

Three materials are used in this study: a *microplane material model for concrete*, a *microplane smeared bond material model* and a *tri-linear steel material model*. A brief discussion of these material models for 3D cyclic analysis is presented in this section.

Microplane model

The microplane model is a three-dimensional, macroscopic model in which the material is characterized by uniaxial relations between the stress and strain components on planes of various orientations. At each element integration point these “microplanes” can be imagined to represent damage planes or weak planes of the microstructure (see Figure 1a). In the model the tensorial invariance restrictions need not be directly enforced. They are automatically satisfied by superimposing the responses from all microplanes in a suitable manner.

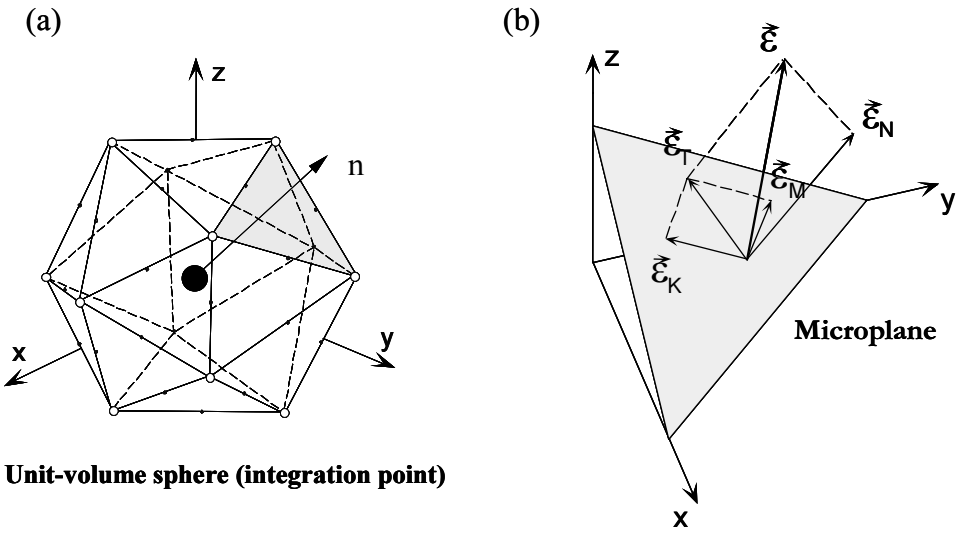

Figure 1. Microplane model: (a) Integration sphere; (b) Microplane stress-strain components

Ožbolt et al. recently proposed an advanced version of the microplane model for concrete [Ožbolt et al. 2001]. This model is based on the so-called "relaxed kinematic constraint" concept. In the model, the microplane is defined by its unit normal vector of components n_i (see Figure 1b). Normal and shear stress and strain components (σ_N, σ_{Tr}; ε_N, ε_{Tr}) are considered on each plane. Microplane strains are assumed to be the projections of the macroscopic strain tensor ε_{ij} (kinematic constraint). Based on the virtual work approach, which represents a weak form of the equilibrium between macroscopic response and microplane responses, the macroscopic stress tensor is obtained as an integral over all possible, previously defined, microplane orientations:

$$\sigma_{ij} = \frac{3}{2\pi}\int_{\Omega}\sigma_N n_i n_j d\Omega + \frac{3}{2\pi}\int_{\Omega}\frac{\sigma_{Tr}}{2}(n_i\delta_{rj} + n_j\delta_{ri})\ d\Omega \tag{1}$$

To realistically model concrete, the normal microplane stress and strain components must be decomposed into volumetric and deviatoric parts ($\sigma_N=\sigma_V+\sigma_D$, $\varepsilon_N=\varepsilon_V+\varepsilon_D$; see Figure 1), which leads to the following expression for the macroscopic stress tensor:

$$\sigma_{ij} = \sigma_V\delta_{ij} + \frac{3}{2\pi}\int_{\Omega}\sigma_D n_i n_j\, d\Omega + \frac{3}{2\pi}\int_{\Omega}\frac{\sigma_{Tr}}{2}(n_i\delta_{rj} + n_j\delta_{ri})\, d\Omega \tag{2}$$

For each microplane component the uniaxial stress-strain relations are assumed as:

$$\sigma_V = F_V(\varepsilon_{V,eff}) \;\; ; \quad \sigma_D = F_D(\varepsilon_{D,eff}) \;\; ; \quad \sigma_{Tr} = F_{Tr}(\varepsilon_{Tr,eff}, \varepsilon_{V,eff}) \tag{3}$$

The microplane strains are calculated from the macroscopic strain tensor based on the kinematic constraint approach. In Eq. (3), however, only effective parts of these strains are used to calculate microplane stresses (relaxation of the kinematic constraint). The macroscopic stress tensor is obtained from Eq. (2) in which the integration over all microplane directions (21 directions) is performed numerically.

To model unloading, reloading and cyclic loading for general triaxial stress-strain states, loading and unloading rules for each microplane stress-strain component are introduced. The "virgin loading" for each microplane strain component occurs if:

$$\varepsilon \Delta\varepsilon \geq 0 \quad \text{and} \quad (\varepsilon - \varepsilon_{\max})(\varepsilon - \varepsilon_{\min}) \geq 0 \tag{4}$$

where ε_{max} and ε_{min} are the maximum and minimum values of the effective microplane strain that have occurred so far; otherwise unloading or reloading takes place. In contrast to virgin loading, for cyclic loading the stress-strain relations must be written in the incremental form:

$$d\sigma = E d\varepsilon \tag{5}$$

where E represents unloading-reloading tangent modulus, which is generally defined as:

$$\begin{aligned} &E = E_0\alpha + \sigma\left(\frac{1-\alpha}{\varepsilon - \varepsilon_1}\right) \\ &\varepsilon > \varepsilon_P; \qquad \varepsilon_1 = \varepsilon_P - \frac{\sigma_P}{E_0} + \beta(\varepsilon - \varepsilon_P) \\ &\varepsilon \leq \varepsilon_P; \qquad \varepsilon_1 = 0 \end{aligned} \tag{6}$$

In Eq. (6) σ_p and ε_p denote the positive or negative peak stress and the corresponding strain for each microplane component using values σ_p^+, ε_p^+ and σ_p^-, ε_p^- for positive and negative peaks, respectively. The constants α and β are

empirically chosen ranging between 1 and 0 and E_0 is the initial elastic modulus for the corresponding microplane component.

The loading-unloading-reloading rules for microplane components are schematically plotted in Figure 2. Figure 2a shows rules for cyclic behaviour of the volumetric stress-strain component. In the compressive region the loading-unloading modulus is defined by the initial elastic modulus $E_{V,0}$. For tension, the unloading and reloading moduli are controlled by Eq. (6). The typical load cycle for virgin loading in tension, unloading in compression and subsequent reloading in tension is: 0-P-A-B-C-D-A-B-E-F-0-A. Virgin loading in compression, unloading and subsequent loading in tension follows the path: 0-A'-B'-D'-A' or 0-A'-B'-0-P-A-B-E-F-0-A (Figure 2a). For the deviatoric compression and tension similar rules to those for the volumetric tension are employed (see Figure 2b). The loading-unloading-reloading rules for shear are principally the same as for the deviatoric component.

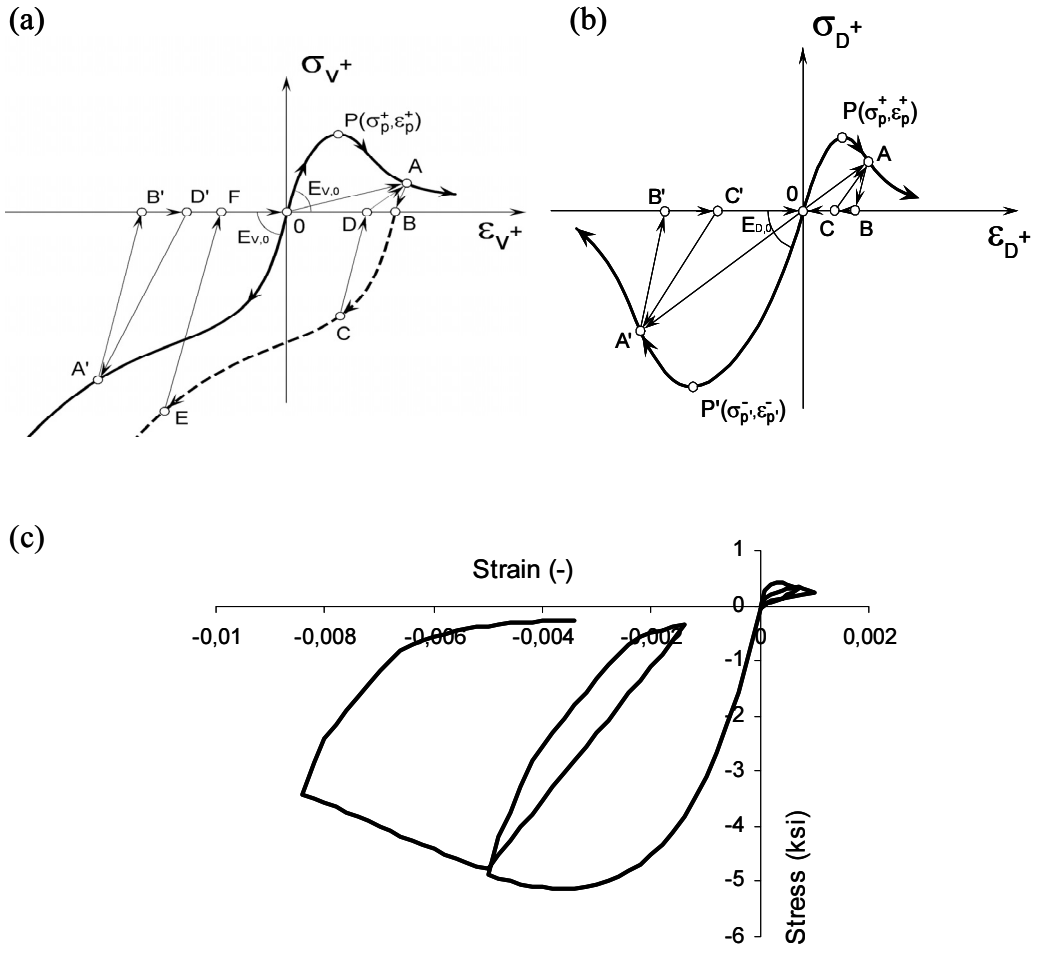

Figure 2. Cyclic stress-strain relationship: (a) Volumetric microplane component; (b) Deviatoric microplane component; (c) Macroscopic response – unit 3D FE under uniaxial tension-compression load history

The general three-dimensional cyclic response resulting from several one-dimensional microplane responses (see Figure 2c) is an important feature of the model. The relatively simple cyclic rules allow us to better understand the macroscopic material response and to correlate it with the material structure and macroscopic stress and strain tensor. The verification of the above-mentioned cyclic rules is shown in [Ožbolt et al. 2001]. It is demonstrated that the model is able to realistically simulate the concrete cyclic stress-strain response for a general loading history.

Bond Model

The bond between reinforcement and concrete can be modelled using either a smeared or a discrete approach. In the present analysis the bond is represented by a layer of 3D elements around the reinforced bar, i.e. smeared approach is employed. The microplane material model was adapted for these elements such that the shear stress-strain relationship yielded a realistic shear stress-slip relation. The slip is obtained by multiplying the shear strains by the element depth, i.e. by the thickness of the finite elements located around the reinforcement. The shear stress-slip relationship used for the present case studies is plotted in Figure 3. One should note that the model does not account for stiffness and strength reduction for unloading and reloading in the opposite direction, i.e. the relation is symmetric. The bond strength and stiffness is, however, reduced with repeated cycling due to accumulation of damage in the material.

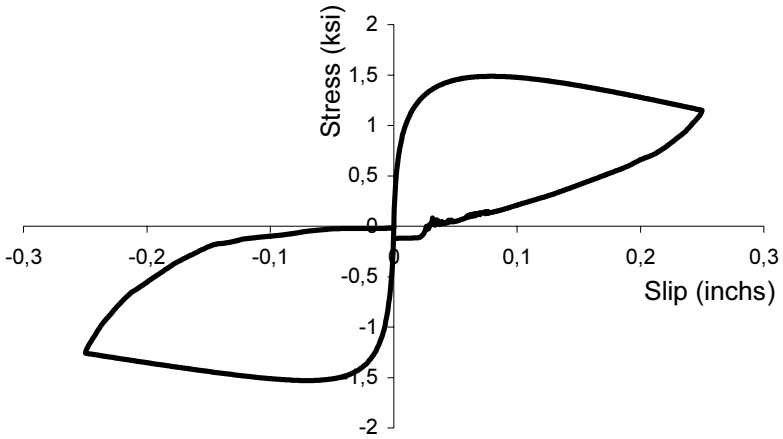

Figure 3. Shear stress-slip relation used to represent bond

Reinforcement Steel

A simple tri-linear cyclic material was used to represent the steel reinforcement. The skeletal curve for this material is shown in Figure 4. The material is a corrected version of the previous steel material used in MASA. The Bauschinger effect was ignored in the model.

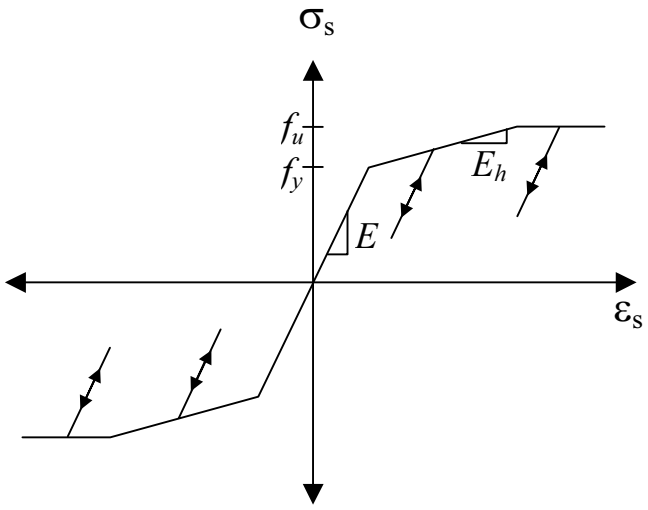

Figure 4. Tri-linear cyclic steel material model

Localization Limiter - Crack Band Method

A crack band localisation limiter is used with the 3D elements. A critical assumption of the crack band method is that damage (i.e. cracks) localizes in a row of finite elements. To assure a constant and mesh independent energy consumption capacity for concrete (concrete fracture energy G_F), the constitutive law needs to be adapted such that:

$$G_F = A_f h = const. \tag{7}$$

where $A_f =$ the area under the uniaxial tensile stress-strain curve and $h =$ width of the crack band (average element size). The same relation is valid for uniaxial compression (no lateral confinement) with the assumption that the concrete compressive fracture energy G_C is a material constant:

$$G_C = A_{fc} h = const. \tag{8}$$

in which A_{fc} = area under the uniaxial compressive stress-strain curve. In the present numerical study it is assumed that G_C is approximately 200 times larger than G_F ($G_C \approx 200 \cdot G_F$).

TEST SPECIMENS AND FINITE ELEMENT MODEL

The specimens used for this numerical study were selected from a series of experimental tests performed during the late 1960's and early 1970's at the University of California, Berkeley. Members from this test program were chosen because: 1) relatively simple member geometries representative of 'typical' building details for the time were used, 2) examples of members designed for both flexure and shear failure were investigated, 3) the members were detailed to minimized the unwanted effects of reinforcement slip in the column and 4) extensive documentation of both global (load-displacement) and local (cracking) behaviour was maintained.

Analyses of flexural beam members R-3 and R-4 investigated by Ma et al. [Ma et al. 1976] are presented in the present paper. These beams are rectangular members adapted to represent the critical region at a beam-column interface in a lower exterior girder of a 20-story ductile moment-resisting concrete frame. The only differences between beam R-3 and R-4 were the cyclic loading history applied and a slight difference in the concrete compressive strength. Details for the beams are shown in Figure 5.

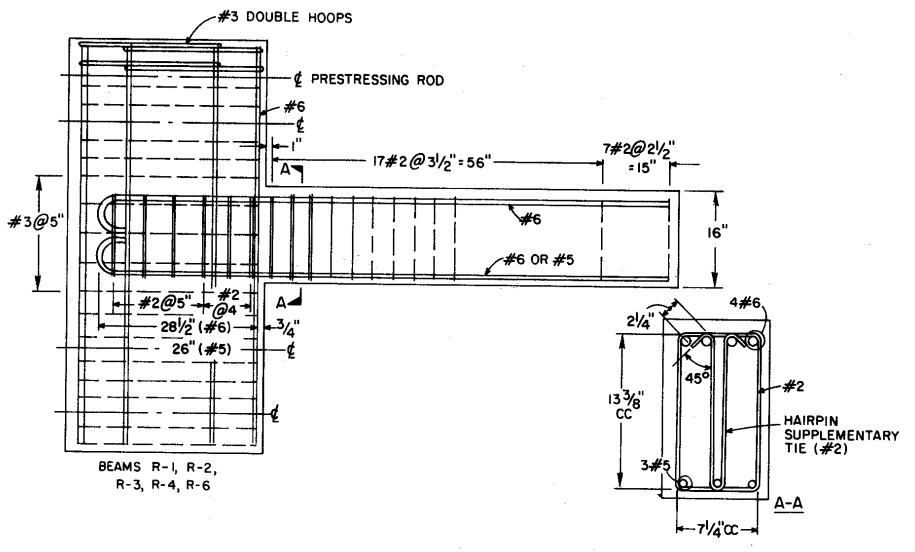

Figure 5. Reinforcement details

A detailed 3D finite element mesh was prepared using the mesh generation program FEMAP. The mesh in Figure 6, shown in section to illustrate the significant features of the model, is the result of several iterations to determine the necessary mesh configuration. For the analyses, the X-axis symmetry of the structure was exploited to reduce the number of elements.

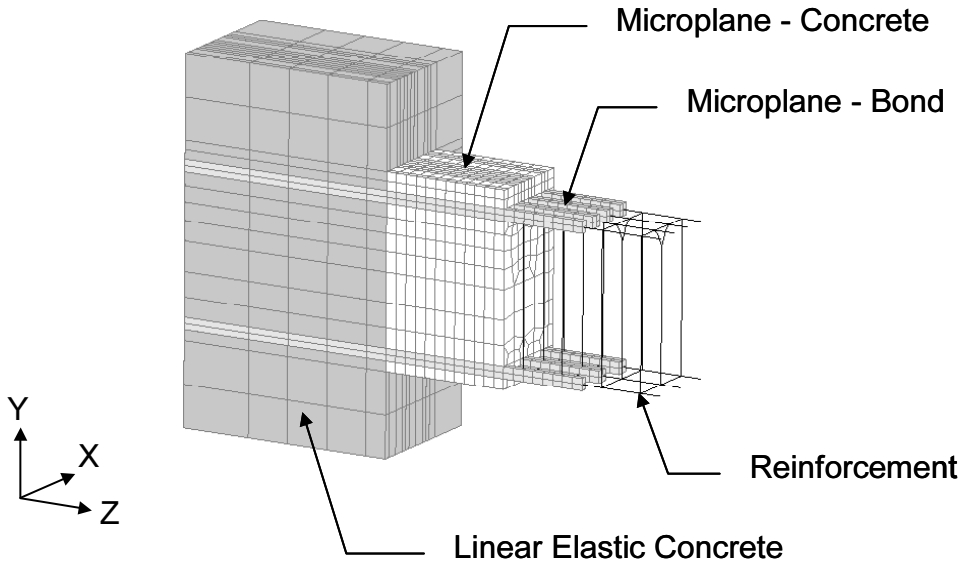

Figure 6. Section of the 3D finite element mesh for beams R-3 and R-4

The original mesh was significantly less detailed than that shown in Figure 6. A simple fixed-end cantilever without a bond material was used. It was discovered during the analysis, however, that oversimplification of the model yielded a significantly different failure mechanism. The support end of the member and the region of load application were particularly important. Figure 7 shows the difference in the monotonic load-displacement curves for models with and without modelling of the support block. The difference in the two curves is caused by a shift in the onset of a shearing mechanism in the member. The fixed restraint prematurely initiates shearing in the member. A further improvement, in the sense of better representation of the experimental results, was obtained when the steel material was corrected to account for post-yield hardening.

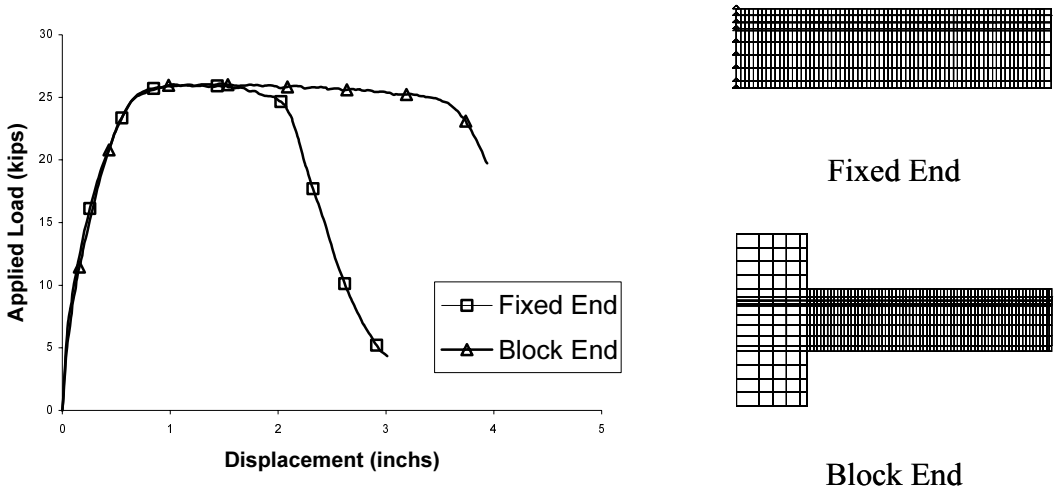

Figure 7. Influence of modelling the support structure

We found that providing a bond material for the elements surrounding the longitudinal reinforcing steel (See Figure 6) improved the cyclic performance by "relaxing" the continuum in this region. There are two effects contributing to this improved performance. The first is that in modelling bond we provided smaller elements at the steel-concrete interface and thus achieved a better representation of cracking in this critical zone. The second effect is that the bond material somewhat decoupled the deformation of the steel from the concrete continuum. This allowed cracks that were opened in the tension region of the member during loading in one direction to close earlier after load reversal.

Another critical location in the model is the point of load application. Load was applied to the member by means of a pin-type connection, i.e. free rotation, at the beam tip. Because highly localized shear stresses can occur at the point of load application, we had to use a linear elastic concrete material with the geometry shown in Figure 8 to reduce the formation of shear cracks along a single row of elements during cycling. This problem could also be avoided using contact elements, however, the contact element is not currently implemented in the cyclic version of MASA.

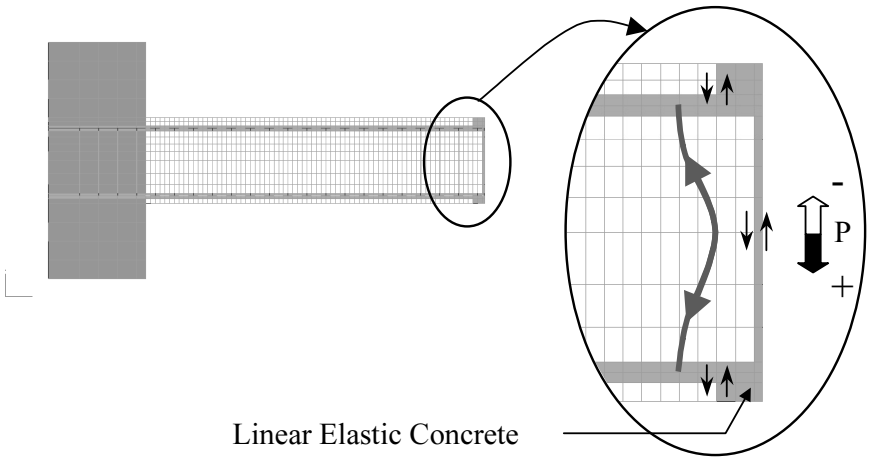

Figure 8. Shear flow at point of load application

All analyses were displacement controlled. Positive loading is considered to be downward bending of the beam as shown in Figure 8. The applied displacement histories shown in Figure 9 were generated based on the information provide in [Ma et al. 1976]. It is noted that the applied displacement histories were not exactly the same as those used in the experiments because the initial stages of the cyclic history in the experiment were force controlled and determined during the test based on observed cracking in the member. The displacement values obtained during these cycles are not always explicitly provided and thus it was necessary to generate parts of the early portion of the input displacement histories from experimental data by eye. The differences, however, are on the order of fractions of an inch and deemed to be insignificant.

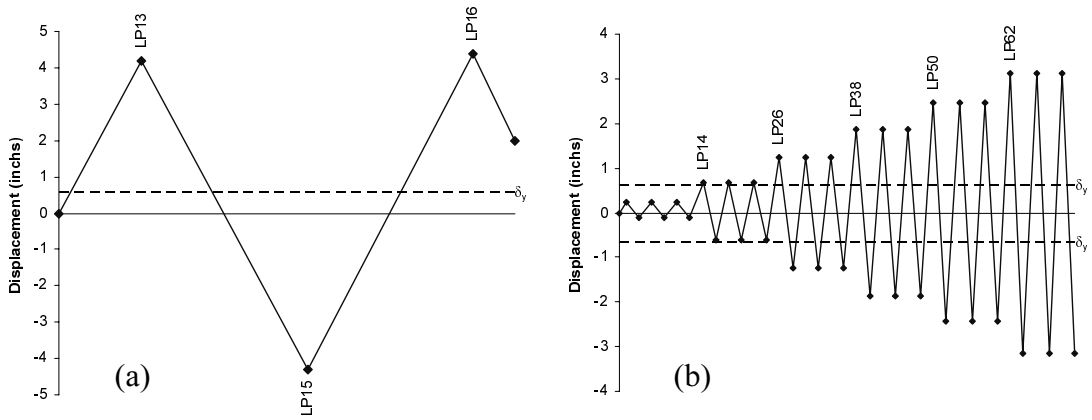

Figure 9. Applied displacement time-histories: (a) Beam R-4; (b) Beam R-3

The “LP” designations in Figure 9 are load control points used during the experimental tests and are applied in this paper as reference points. The numbering scheme is arbitrary with respect to the numerical study.

Early on in the study it was discovered that MASA must be executed using a Constant Stiffness Method (CSM) approach for nonlinear iterations when cyclic analysis is conducted. When a Tangent Method (TM) or Secant Stiffness Method (SSM) is used, the program often ‘hangs’ when attempting to cross the point of zero applied load after the beam has been damaged (See Figure 10). This is believed to happen because the severely damaged cover concrete makes the iterated stiffness ill-conditioned. The concrete cover, however, does not significantly affect the global member behaviour.

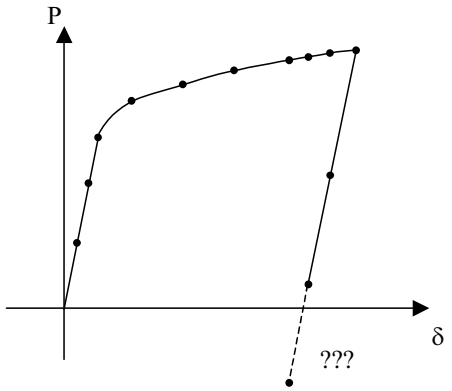

Figure 10. Schematic of problematic location during nonlinear reversed-cyclic analysis

ANALYSIS OF RESULTS AND COMPARISON WITH EXPERIMENTAL DATA

In this section numerical results obtained using MASA are presented along with selected experimental data.

Figure 11 shows cracking and the distribution of strains in the reinforcing steel in beam R-4 shortly after yielding during the “virgin” loading of the member. In Figure 11b one can see the distribution of strain in the reinforcement between cracks. Unfortunately, experimentally measured steel strain distributions for the members we analysed were not available for comparison. The crack building process in the concrete, however, is an essential feature of the “linear elastic” load-displacement behaviour and is captured by MASA.

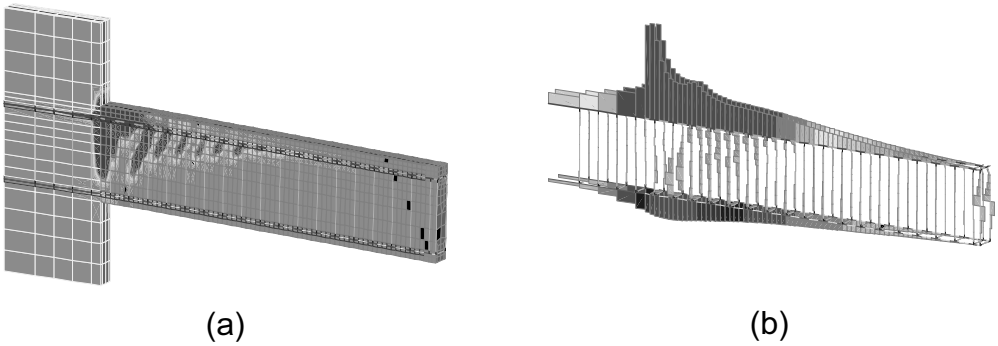

Figure 11. Virgin loading of beam R-4: (a) Principle strains; (b) Axial strain in reinforcement

The load-displacement response is a useful tool to evaluate the ability of MASA to represent the real behaviour of the members. Figure 12 and Figure 13 compare the load-displacement response at the member tip obtained from the numerical and experimental tests. Although the terminology "Applied Load" is used to coincide with the data presented in the experimental report, it is reiterated that all of the analyses using MASA were carried out under displacement control.

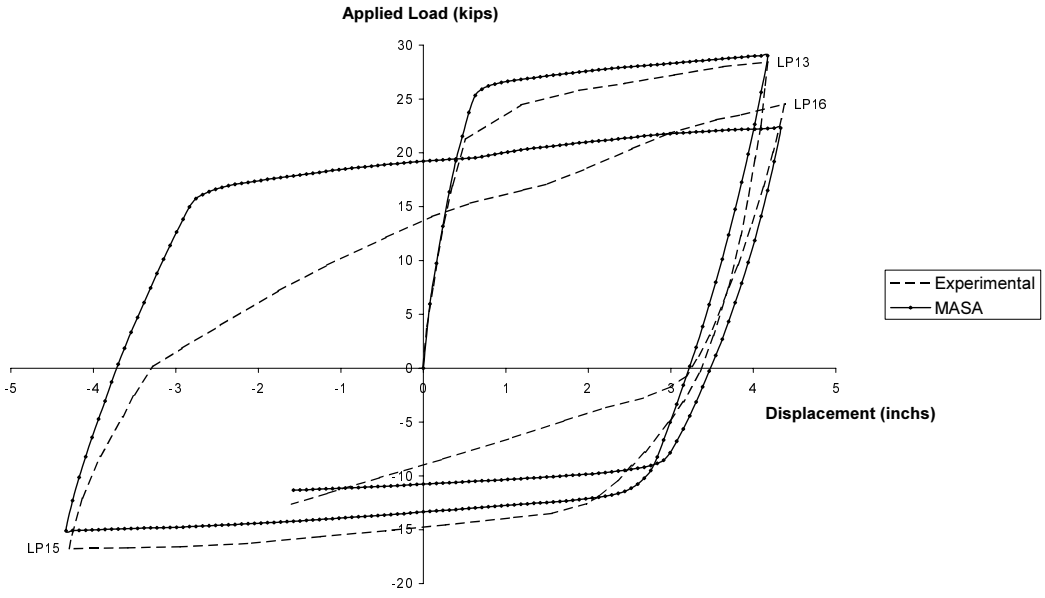

Figure 12. Load-displacement diagram for beam R-4

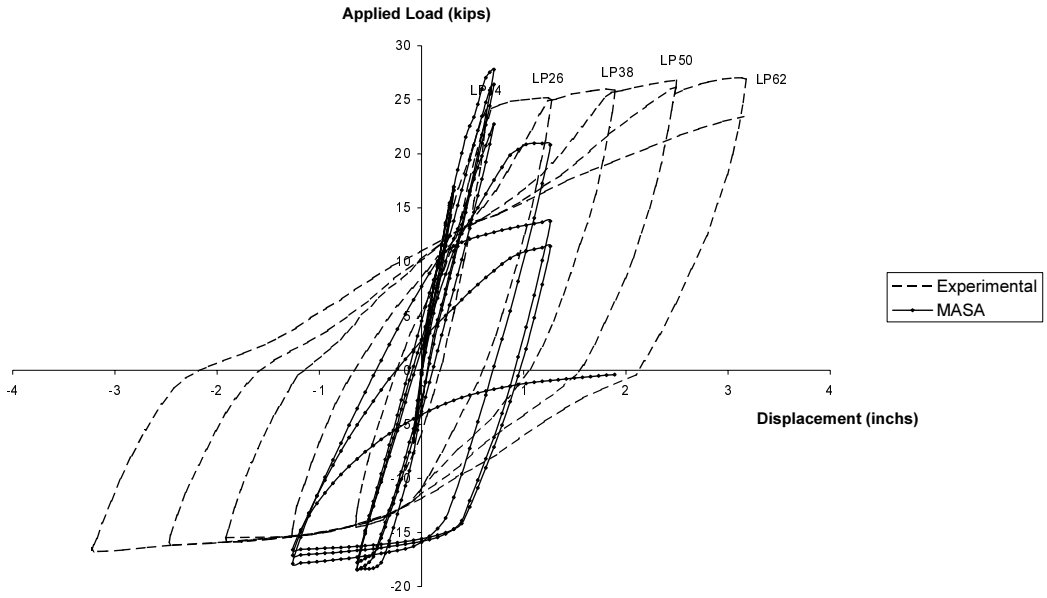

Figure 13. Load-displacement diagram for beam R-3

The figures show that the hysteretic behaviour is quite well represented for member R-4, however, there is a significant divergence from the experimental results for multiple reversed cycling over the yield point in member R-3. The analysis of R-3 was terminated at the fourth displacement plateau (LP38) because the member had clearly failed.

We concentrate our discussion on member R-4 because the mechanism that led to the failure of member R-3 in our numerical analysis was also present in the analysis of member R-4, however, its contribution to the ultimate failure was less pronounced for the case with a lower number of cycles.

Figure 14 shows the computed deformations and principal strains for member R-4 at the points of load reversal. The principal strains provide a picture of cracking in the member. Figure 14a shows that the deformation up to the first load reversal is primarily flexural. At the second load reversal (Figure 14b) one observes significant shear deformation in the member. This shear deformation is also seen in the subsequent load reversals (Figure 14c and Figure 14d).

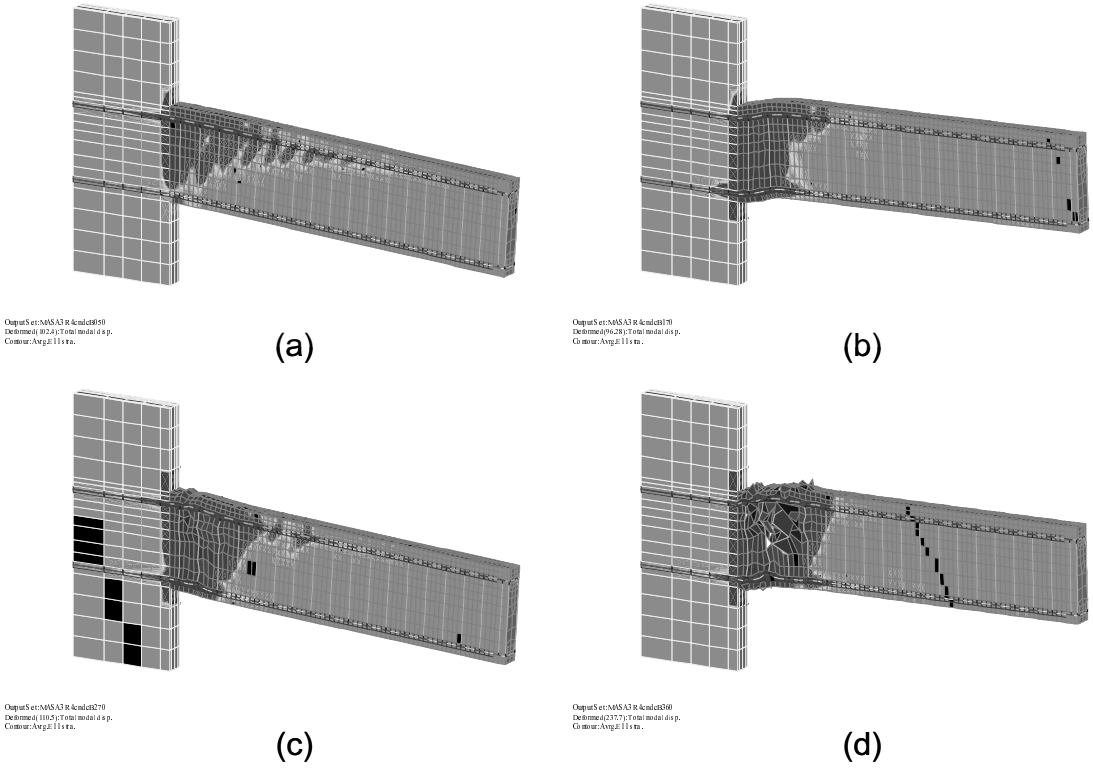

Figure 14. Principal strains in beam R-4: (a) LP13; (b) LP15; (c) LP16; (d) Failure

Localized shearing was a concern during the experimental investigations as well, as demonstrated by the fact that shear behaviour was monitored even for the so-called "flexural members" R-3 and R-4. This provides us the opportunity to more closely examine shearing in the members. An illustration of how an average shear angle was measured in the experiments and subsequently in our finite element analyses is shown in Figure 15.

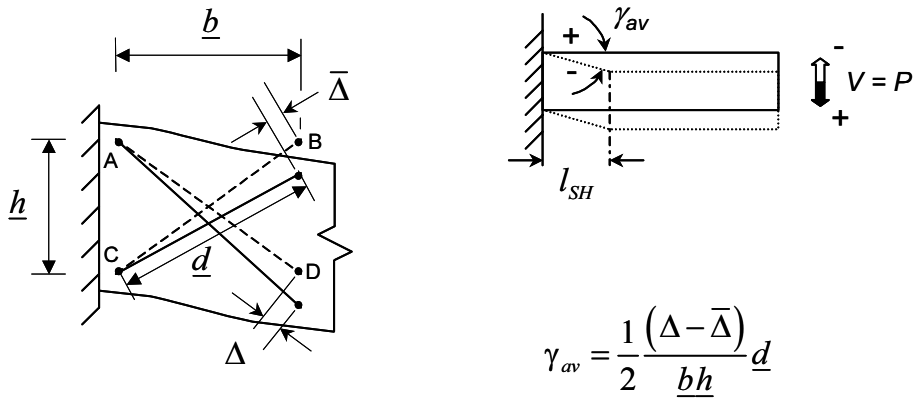

Figure 15. Description of average shear angle γ_{av}

Figure 16 shows the applied load plotted against the shear distortion for member R-4. While the agreement of the numerical and experimental results is quite good up to control point LP13, the shear distortion observed after the first load reversal reaches a value nearly 3 times that of the experimental. This confirms what is observed in Figure 14a through Figure 14d. It is this shear deformation that leads to the early degradation of member R-3. The material damage caused by this shearing is more pronounced for the case with a higher number of cycles.

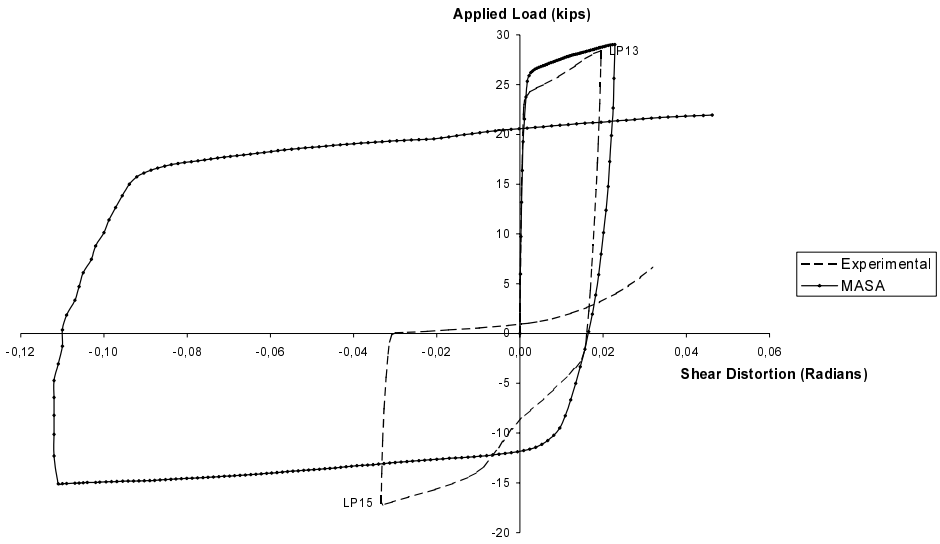

Figure 16. Load-shear distortion diagram for beam R-4

Throughout the study MASA was seen to be sensitive to material damage caused by shearing. In actual reinforced concrete members where simultaneous flexure and shear are present, shear forces are transferred by three mechanisms: 1) shear transfer across concrete in compression, 2) dowel action across cracks by reinforcement and 3) mechanical interlock along crack surfaces. In MASA shear is transferred primarily by the concrete in compression.

Due to constraints in MASA we were required to use either truss elements or fixed-end beam elements (See Figure 17) to model the reinforcing steel because no rotational degree of freedom exists in the element formulations.

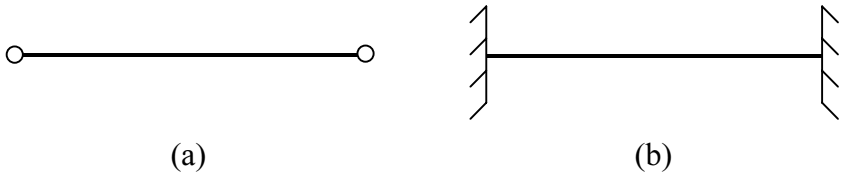

Figure 17. Reinforcement elements in MASA: (a) Truss; (b) Fixed-end beam

We eventually constructed an element for the reinforcement that acted in tension as a truss and in compression as a fixed-end beam with a flexural stiffness based on $1/100^{th}$ the moment of inertia. This provided the reinforcement with some rigidity in compression, which prevented "kinking" of the reinforcement, without artificially stiffening the member. This solution does not, however, allow for shear transfer through dowel action.

It is possible that including the Bauschinger effect in the steel material model would help reduce shear sensitivity in MASA during cycling. By adding the Bauschinger effect, which expedites the onset of re-yielding of the steel (See Figure 18), cracks in the concrete would be able to close more easily, thus allowing for a compression zone to develop where shears could be transferred. The absence of the Bauschinger effect in the current MASA version can also be observed as the discrepancy between experimental and numerical results in the load-displacement curve in Figure 12.

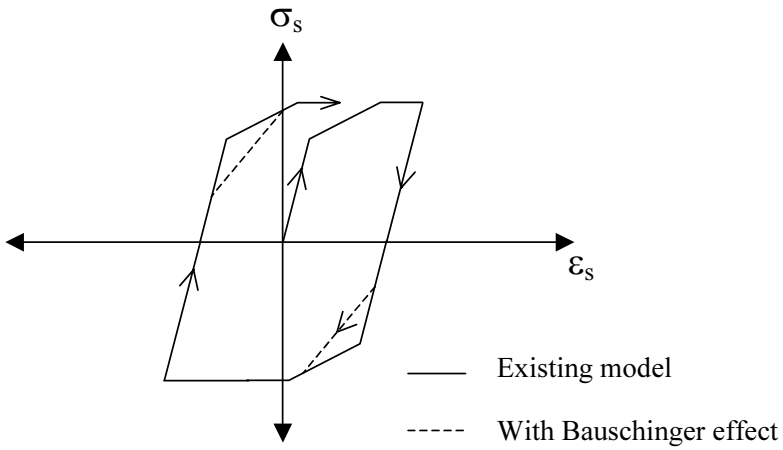

Figure 18. Schematic of Bauschinger effect on steel stress-strain curve

Extensive photographic records were maintained during the experimental investigations. A qualitative comparison of the crack patterns for members R-4 and R-3 is shown in Figure 19 and Figure 20, respectively.

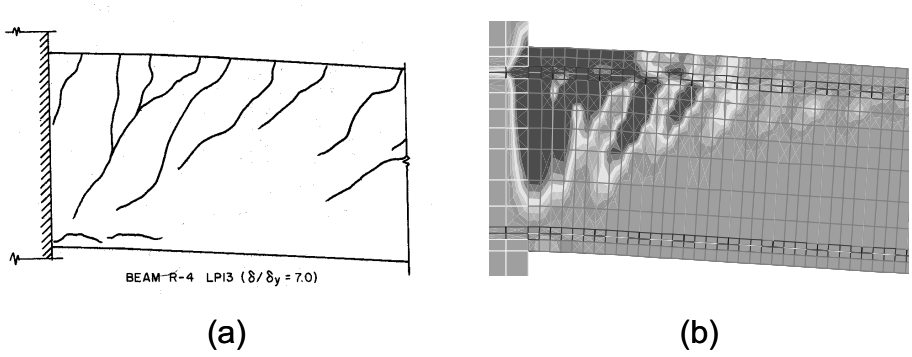

Figure 19. Crack patterns in beam R-4: (a) Experimental, $\delta/\delta_y = 7.0$; (b) MASA, $\delta/\delta_y = 7.0$

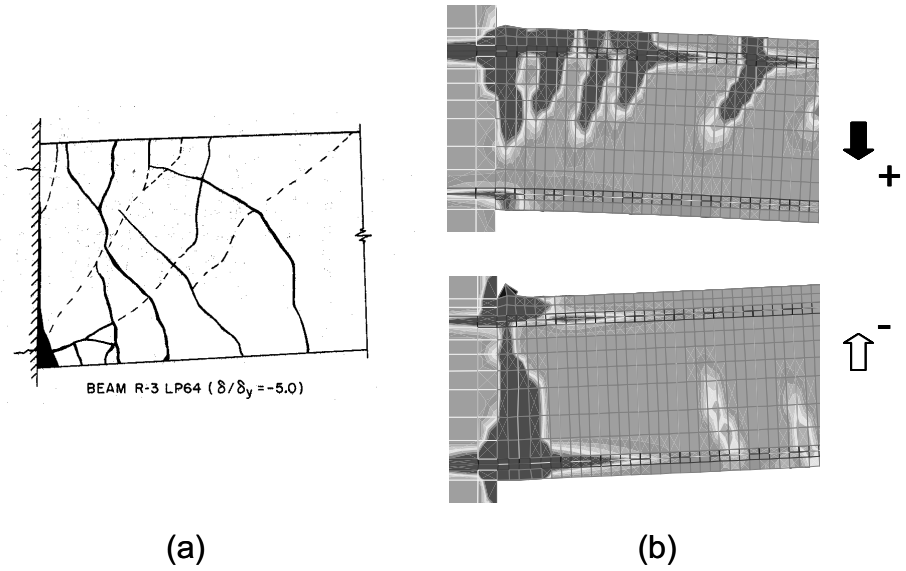

Figure 20. Crack patterns in beam R-3: (a) Experimental, $\delta/\delta_y = 5.0$; (b) MASA, $\delta/\delta_y = 1.0$

In the experiments the ultimate failure mode for both members R-3 and R-4 was blowout of the concrete in compression and a buckling of the longitudinal reinforcement. This failure mode was observed in the numerical investigations for member R-4 as shown in Figure 21.

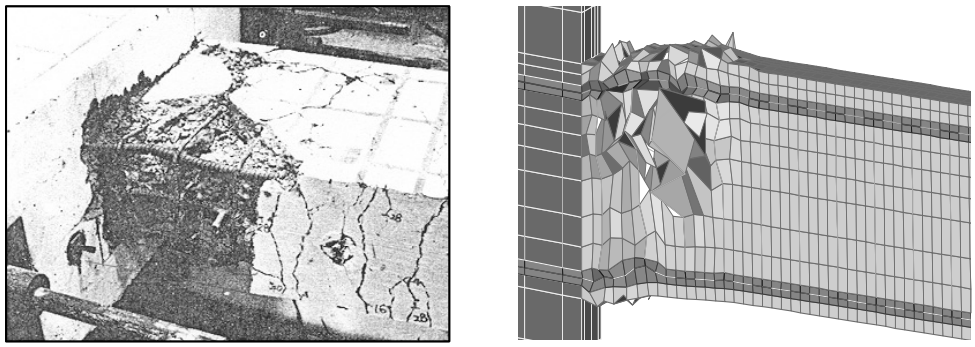

Figure 21. Ultimate failure mode: (a) Experimental (Beam R-3); (b) MASA (Beam R-4)

CONCLUSIONS

In this paper the present capacity of the microplane based finite element program MASA for nonlinear, three-dimensional, reversed-cyclic analysis of reinforced concrete members is presented.

A finite element model developed to study beam members R-3 and R-4 from the experiments by Ma et al. is discussed. For three-dimensional cyclic modelling, correct representation of the boundary conditions, both at the support and at the loading point, is essential to recover the proper failure mode. Furthermore, a bond material is needed to "relax" the continuum at the steel-concrete interface. An additional consequence of working within a continuum framework is that "spalled" concrete cover leads to local numerical instabilities. These instabilities do not, however, have a significant influence on the overall load-displacement behaviour of the member. We reduced this problem by providing the concrete material with a high ductility to prevent elements from "flying away". A Constant Stiffness Method (CSM) for the nonlinear iterations was required for cyclic analysis.

MASA is shown to represent global hysteretic behaviour, as long at the number of cycles is limited. Shear sensitivity continues to be a problem and can lead to premature failure for repeated cycling. The program realistically represents cracking and provides useful qualitative and quantitative information on crack formation in the concrete and strain distribution in the reinforcement.

In the future, reinforcement elements with rotational degrees of freedom would likely reduce the shear problem by providing a dowel effect. Adding the Bauschinger effect for the steel model would require only a simple modification

and could significantly improve overall performance. A discrete bond material would furtherer improve the cyclic behaviour in MASA by separating the reinforcement elements from the continuum material formulation. Furthermore, the bond relation should account for bond degradation during load reversals, i.e. the bond relation should have asymmetry dependent on the load history.

REFERENCES

Ožbolt, J.; Li, Y.-J.; Kožar, L., "Microplane Model for Concrete with Relaxed Kinematic Constraint", International Journal of Solids and Structures, Vol. 38, 2001, pp. 2683-2711

EDF – Elecricité de France, MECA Benchmark – Three Dimensional Non Linear Constitutive Models of Fractured Concrete: Evaluation – Comparison – Adaptation, Comparison Report #1 (draft report), March 2001

Ožbolt, J.; Meštrović, D.; Li, Y.-J.; Eligehausen, R., "Compression Failure of Beams Made of Different Concrete Types and Sizes", Journal of Structural Engineering, ASCE, Vol. 126, No. 2, February, 2000, pp. 200-209

Ožbolt, J.; Li, Y.-J.; Eligehausen, R., "3D Cyclic Finite Element Analysis of Beam-Column Connections", Fracture Mechanics of Concrete Structures, Vol. 3, 1998, pp. 1523-1536

Ma, S.-Y. M.; Bertero, V. V.; Popov, E. P., Experimental and Analytical Studies on the Hysteretic Behaviour of Reinforced Concrete Rectangular and T-beams, Earthquake Engineering Research Center (EERC), Report No. UBC/EERC 76-2, University of California, Berkeley, 1976